Defining Top-of-the-Atmosphere Flux Reference Level for Earth Radiation Budget Studies

NORMAN G. LOEB AND SEIJI KATO

Center for Atmospheric Sciences, Hampton University, Hampton, Virginia

BRUCE A. WIELICKI

NASA Langley Research Center, Hampton, Virginia

(Manuscript received 11 February 2002, in final form 12 June 2002)

ABSTRACT

To estimate the earth's radiation budget at the top of the atmosphere (TOA) from satellite-measured radiances, it is necessary to account for the finite geometry of the earth and recognize that the earth is a solid body surrounded by a translucent atmosphere of finite thickness that attenuates solar radiation differently at different heights. As a result, in order to account for all of the reflected solar and emitted thermal radiation from the planet by direct integration of satellite-measured radiances, the measurement viewing geometry must be defined at a reference level well above the earth's surface (e.g., 100 km). This ensures that all radiation contributions, including radiation escaping the planet along slant paths above the earth's tangent point, are accounted for. By using a field-of-view (FOV) reference level that is too low (such as the surface reference level), TOA fluxes for most scene types are systematically underestimated by 1–2 W m^{-2}. In addition, since TOA flux represents a flow of radiant energy per unit area, and varies with distance from the earth according to the inverse-square law, a reference level is also needed to define satellite-based TOA fluxes. From theoretical radiative transfer calculations using a model that accounts for spherical geometry, the optimal reference level for defining TOA fluxes in radiation budget studies for the earth is estimated to be approximately 20 km. At this reference level, there is no need to explicitly account for horizontal transmission of solar radiation through the atmosphere in the earth radiation budget calculation. In this context, therefore, the 20-km reference level corresponds to the effective radiative ''top of atmosphere'' for the planet. Although the optimal flux reference level depends slightly on scene type due to differences in effective transmission of solar radiation with cloud height, the difference in flux caused by neglecting the scene-type dependence is less than 0.1%. If an inappropriate TOA flux reference level is used to define satellite TOA fluxes, and horizontal transmission of solar radiation through the planet is not accounted for in the radiation budget equation, systematic errors in net flux of up to 8 W m^{-2} can result. Since climate models generally use a plane-parallel model approximation to estimate TOA fluxes and the earth radiation budget, they implicitly assume zero horizontal transmission of solar radiation in the radiation budget equation, and do not need to specify a flux reference level. By defining satellite-based TOA flux estimates at a 20-km flux reference level, comparisons with plane-parallel climate model calculations are simplified since there is no need to explicitly correct plane-parallel climate model fluxes for horizontal transmission of solar radiation through a finite earth.

1. Introduction

Since the launch of the first satellite instruments there has been much interest in determining radiative fluxes at the top of the atmosphere (TOA) for earth radiation budget studies (House et al. 1986). To obtain reflected shortwave (SW; or solar) and emitted longwave (LW; or thermal infrared) TOA fluxes from narrow field-of-view (FOV) scanning radiometers, the measured radiance in a particular sun–earth–observer viewing geometry is converted to a TOA flux using anisotropic correction factors that account for the angular dependence of the radiation field. The Earth Radiation Budget Experiment (ERBE; Barkstrom 1984) used a set of 12 angular distribution models (ADMs) to determine radiative fluxes under clear, partly cloudy, mostly cloudy, and overcast conditions over ocean, land, desert, and snow (Suttles et al. 1988, 1989). The Clouds and the Earth's Radiant Energy System (CERES) will combine SW, LW, and window (WN) radiance measurements with high-resolution imager-based cloud retrievals to significantly increase the scene-type stratification of CERES ADMs (Wielicki et al. 1996).

One of the more subtle issues that arise when analyzing satellite data is the need to specify the reference level of measured and derived quantities. Here two ref-

Corresponding author address: Dr. Norman G. Loeb, NASA Langley Research Center, Mail Stop 420, Hampton, VA 23681-2199.
E-mail: n.g.loeb@larc.nasa.gov

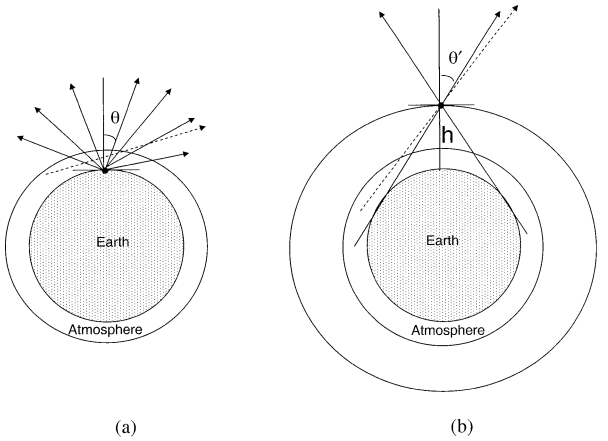

FIG. 1. Schematic diagram illustrating how viewing geometry changes with FOV reference level. (a) When the FOV reference level is at the surface, radiance contributions from slant paths through the atmosphere emerging beyond the earth's tangent point are unaccounted for (dashed line). (b) If the reference level is raised to a height *h* above the surface, off-earth view radiance contributions are accounted for.

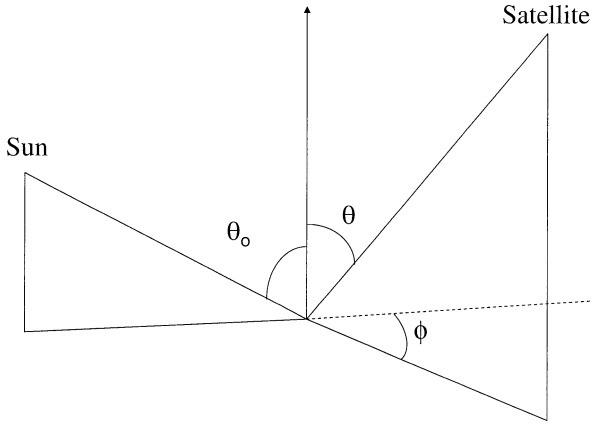

FIG. 2. Illustration of sun–earth–observer viewing geometry.

erence levels are considered: (i) the ''field-of-view (FOV)'' reference level, which defines the level where a measurement's sun–earth–observer viewing geometry is defined; and (ii) the ''flux'' reference level, which defines the reference level where TOA fluxes are defined. Remote sensing applications commonly define the FOV reference level at the earth's surface. An exception is the Multi-angle Imaging Spectroradiometer (MISR; Diner et al. 1999), which adjusts the FOV reference level to the height from where the radiation is reflected (e.g., cloud top). In order to determine the TOA flux by explicit integration of upwelling measured radiances, all of the outgoing radiation from the earth–atmosphere must be accounted for. This includes radiance contributions from slant paths emerging from beyond the earth's horizon (dashed line in Fig. 1a). To account for this energy, the FOV reference level must be defined high enough above the earth's surface (Fig. 1b).

The flux reference level arises from the notion of flux as outgoing (SW or LW) radiant energy through a spherical surface surrounding the earth–atmosphere divided by the surface area of the sphere. If all of the outgoing radiant energy reflected or emitted from the sphere is accounted for (e.g., by selecting a suitable FOV reference level), the flux at any reference level can be determined from the inverse-square law. Previous earth radiation budget (ERB) experiments have selected the flux reference level rather arbitrarily, with little physical justification. The *Nimbus-7* ERB experiment assumed a 15-km flux reference level (Jacobowitz et al. 1984), while ERBE used a 30-km flux reference level (Smith et al. 1986). It is not immediately clear what flux reference level is most appropriate in order to determine the earth's radiation budget. A simple calculation shows that a change in flux reference level from the surface of the earth to a level 30 km above the surface results in a ≈1% decrease in TOA flux, simply due to geometry. This corresponds to a systematic change in the reflected SW and emitted LW fluxes by as much as ≈1 and ≈2.5 W m^{-2}, respectively.

In the following, the importance of selecting appropriate FOV and flux reference levels for estimating the earth's radiation budget from satellite measurements is discussed. To simplify the discussion, the ERBE and CERES methodologies for estimating TOA fluxes from empirical ADMs are used as examples.

2. ADM construction

TOA flux is the radiant energy emitted or scattered by the earth–atmosphere per unit area. Flux is related to radiance (I) as follows:

$$F(\theta_o) = \int_0^{2\pi} \int_0^{\pi/2} I(\theta_o, \theta, \phi) \cos\theta \sin\theta \, d\theta \, d\phi, \quad (1)$$

where θ_o is the solar zenith angle, θ is the observer viewing zenith angle, and ϕ is the relative azimuth angle defining the azimuth angle position of the observer relative to the solar plane (Fig. 2). An ADM is a function that provides anisotropic factors (R) to determine the TOA flux from an observed radiance as follows:

$$F(\theta_o) = \frac{\pi I(\theta_o, \theta, \phi)}{R(\theta_o, \theta, \phi)}. \quad (2)$$

Since only part of the upwelling radiation from a scene can be measured at any given time, F (and R) cannot be measured instantaneously. Instead, R is estimated from a set of predetermined empirical ADMs defined for several scene types with distinct anisotropic characteristics (Suttles et al. 1988, 1989). Each ADM is constructed from a large ensemble of radiance measurements that are sorted into discrete angular bins and parameters that define an ADM scene type. The ADM anisotropic factors for a given scene type (j) are determined from the following:

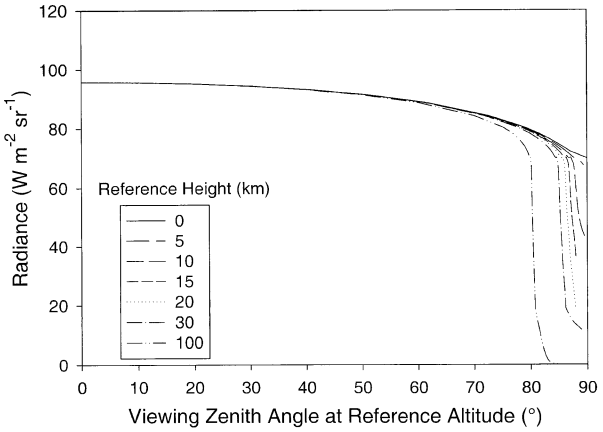

FIG. 3. MODTRAN simulations of broadband LW radiance as a function of viewing zenith angle at different FOV reference levels for a clear ocean scene with a tropical atmosphere and surface temperature of 299.7 K.

$$R_j(\theta_{oi}, \theta_k, \phi_l) = \frac{\pi \bar{I}_j(\theta_{oi}, \theta_k, \phi_l)}{F_j(\theta_{oi})}, \tag{3}$$

where $\bar{I}_j$ is the average radiance (corrected for earth–sun distance in the SW) in angular bin $(\theta_{oi}, \theta_k, \phi_l)$, and F_j is the upwelling flux in solar zenith angle bin θ_{oi}. Here $(\theta_{oi}, \theta_k, \phi_l)$ corresponds to the midpoint of a discrete angular bin defined by $(\theta_{oi} \pm \Delta\theta_o/2, \theta_k \pm \Delta\theta/2, \phi_l \pm \Delta\phi/2)$, where $\Delta\theta_o$, $\Delta\theta$, and $\Delta\phi$ represent the angular bin resolution.

To determine F_j, the usual approach is to explicitly integrate $\bar{I}_j$ using a discrete form of Eq. (1). However, in order to provide an accurate estimate of F_j, all of the reflected or emitted radiant energy from the planet must be accounted for. This includes radiance contributions that emerge from the atmosphere along slant atmospheric paths above the earth's horizon (i.e., above the earth's tangent point). As illustrated in Fig. 1, this is only possible if the observer viewing geometry is defined at a FOV reference level that lies well above the earth's surface.

In order to quantify the contribution of radiances emerging from beyond the Earth's tangent point, MODTRAN (Kneizys et al. 1996) calculations of SW and LW radiances as a function of viewing zenith angle and FOV reference level are considered. MODTRAN is well suited for this problem since it uses spherical geometry to compute the radiances. Figure 3 shows simulations of broadband LW radiance as a function of viewing zenith angle defined at several FOV reference levels. The calculations assume a clear ocean scene with a tropical atmosphere and surface temperature of 299.7 K. Assuming a spherical earth, the viewing zenith angles at two FOV reference levels, h_a and h_b, are related through the law of sines:

$$\sin\theta(h_b) = \left(\frac{r_e + h_a}{r_e + h_b}\right) \sin\theta(h_a), \tag{4}$$

where $\theta(h_a)$ and $\theta(h_b)$ are the viewing zenith angles at reference levels h_a and h_b, respectively, and r_e is the mean radius of the earth (=6371 km). When the FOV reference level in Fig. 3 is well above the earth's surface (e.g., 100 km), radiances decrease to near-zero levels as the viewing zenith angle approaches 90°, and the instrument observes cold space. In contrast, radiances remain large when the FOV reference level is at the surface, even at a viewing zenith angle of 90°.

The error in flux caused by using a FOV reference level that is too low can be estimated by comparing fluxes determined by directly integrating the radiances with fluxes inferred from the inverse-square law. At FOV reference level h, fluxes obtained by direct integration of SW and LW radiances are determined as follows:

$$F_j^{\mathrm{SW}}(\theta_{oi}; h) = \sum_{l=1}^{N_l} w_l \left[\sum_{k=1}^{N_k} w_k \bar{I}_j^{\mathrm{SW}}(\theta_{oi}, \theta_k, \phi_l; h) \cos\theta_k \sin\theta_k\right] \tag{5}$$

$$F_j^{\mathrm{LW}}(h) = 2\pi \sum_{k=1}^{N_k} w_k \bar{I}_j^{\mathrm{LW}}(\theta_k; h) \cos\theta_k \sin\theta_k, \tag{6}$$

where w_k and w_l are Gaussian quadrature weights for integration over viewing zenith angles from 0° to 90°, and relative azimuth angles from 0° to 360°, respectively. Here N_k and N_l represent the number of Gaussian quadrature points (in this study, 200 Gaussian quadrature points are used). The inverse-square law states that the flux varies as the inverse square of the distance from the center of the source (Thomas and Stamnes 1999). It reflects the fact that a change in flux reference level simply changes the surface area over which the outgoing radiant energy is distributed. If the flux is known at one reference level, the flux at any reference level can be determined as follows:

$$F(\theta_o; h_b) = F(\theta_o; h_a)\left(\frac{r_e + h_a}{r_e + h_b}\right)^2, \tag{7}$$

where $F(\theta_o; h_a)$ is the flux at reference level h_a, and $F(\theta_o; h_b)$ is the flux at reference level h_b. If we assume that the flux determined by direct integration at the 100-km FOV reference level accounts for all of the radiation escaping the planet, the flux at any other reference level inferred from the inverse-square law can be compared with the flux determined by direct integration using Eqs. (5) or (6). At a given reference level, the direct integration flux should be the same as that obtained from the inverse-square law. Figure 4 shows results for the clear ocean case in Fig. 3 as a function of reference level. In the figure the LW fluxes evaluated using Eq. (6) are labeled "Direct Integration," and those based on Eq. (7) are labeled "Inverse-Square Law." For reference levels >18 km, fluxes determined by direct integration show an inverse-square law dependence to within 0.1%. Below 18 km, the directly integrated fluxes

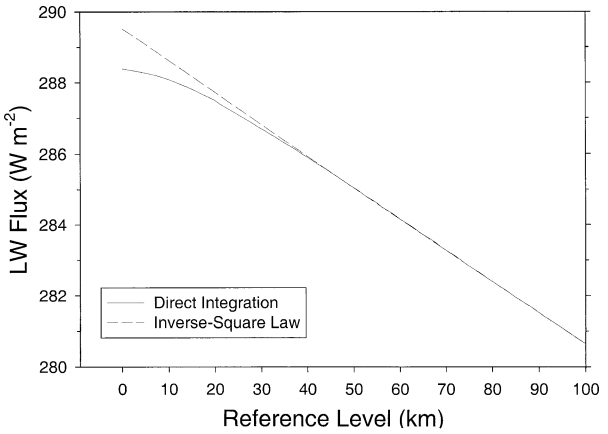

FIG. 4. The LW flux as a function of reference level determined by direct integration of the radiances in Fig. 3 at each FOV reference level (solid line), and by applying the inverse-square law [Eq. (7); dashed line].

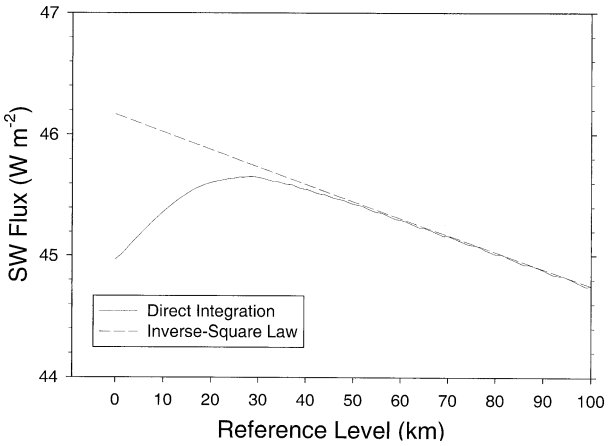

FIG. 5. Same as Fig. 4 but for SW flux at $\theta_o = 45°$ for a clear scene without aerosols (Rayleigh atmosphere) and zero surface reflection.

deviate from the inverse-square law by as much as 0.39% or 1.14 W m^{-2} (at the surface reference level). The direct integration flux at the surface reference level is actually closer to the flux obtained by the inverse-square law at the 13-km reference level. When these calculations are repeated for a 2-km-thick cirrus cloud with a cloud-top height of 9 km (not shown), the deviation from the inverse-square law at the surface reference level is 0.56% or 1.34 W m^{-2}, and the direct integration flux at the surface reference level corresponds more closely with the inverse-square law flux at the 18-km reference level. A further increase in cloud-top height to 15 km increases the flux deviation at the surface reference to 0.92% or 2.17 W m^{-2}, and the direct integration flux at the surface matches the inverse-square law flux at the 30-km reference level.

Figure 5 shows a similar comparison for SW flux at $\theta_o = 45°$ for a clear scene without aerosols (molecular atmosphere) and zero surface reflection. Explicitly integrating radiances using the surface as the FOV reference level leads to an underestimation of the flux by 2.6% or 1.20 W m^{-2}. Interestingly, at reference levels below 30 km, the direct integration flux actually decreases as the reference level decreases. The decrease in flux caused by the ''missing'' radiation at the limb views beyond the earth's horizon more than compensates for the increase in flux that generally accompanies a decrease in flux reference level. The reason the effect is so much more pronounced in the SW than in the LW is because in the SW, radiances generally increase with increasing viewing zenith angle (limb brightening), whereas the opposite (limb darkening) generally occurs in the LW. Thus, the relative error in TOA flux caused by choosing an FOV reference level that is too low is generally larger for the SW than the LW.

From these examples, it is clear that radiance contributions from slant atmospheric paths beyond the earth's tangent point must be accounted for when evaluating Eqs. (5) and (6). However, this is only possible if the measurements at these shallow angles are available from the data product. While satellites routinely measure radiation beyond the earth's horizon, these radiances are not generally processed when the data products are produced. For example, the ERBE and CERES ERBE-like data products retain these footprints, but unfiltered radiances and scene identification at these angles are unavailable. Consequently, some approximations are necessary in order to account for this missing energy.

One approach is to use a radiative transfer model such as MODTRAN to account for radiance contributions at the very large viewing zenith angles. In order to verify that MODTRAN provides an accurate approximation of the flux contribution from radiances emerging from above the earth's tangent point, MODTRAN calculations are compared with 8 months of SW and LW radiance measurements under all-sky conditions from the CERES/Tropical Rainfall Measuring Mission (TRMM) ES8 product. To determine the radiances from the CERES/TRMM ES8 product at angles beyond the earth tangent point, filtered radiances are converted to unfiltered radiances using unfiltering factors provided by Loeb et al. (2001). To simulate the ES8 radiances, the MODTRAN radiances are weighted by the CERES point spread function (Smith 1994). Differences in MODTRAN and ES8 fluxes due to differences in radiance at angles beyond the earth's tangent point are <0.2 W m^{-2}, a factor of 5 reduction in bias compared to that obtained when radiance contributions from these very oblique viewing zenith angles are neglected.

If a 100-km FOV reference level is used to determine the ADM flux F_j, it follows that the ADM can be defined at an arbitrary reference level h as follows:

$$R_j(\theta_{oi}, \theta_k, \phi_l; h) = \frac{\pi \bar{I}_j(\theta_{oi}, \theta_k, \phi_l; h)}{F_j(\theta_{oi}; h_{100})} \left(\frac{r_e + h}{r_e + h_{100}} \right)^2, \quad (8)$$

where $h_{100} = 100$ km.

3. TOA flux reference level

As noted in the preceding section, an instantaneous TOA flux is estimated from an observed radiance measurement by applying an ADM anisotropic correction factor to the radiance measurement [Eq. (2)]. Since a change in flux reference level from the surface to 100 km corresponds to a change in flux of 3% [Eq. (7)], the flux reference level must be clearly specified. Previous radiation budget experiments have been inconsistent in their definition of flux reference level. The *Nimbus-7* ERB experiment assumed a 15-km reference level (Jacobowitz et al. 1984), whereas ERBE used a 30-km reference level (Smith et al. 1986). Furthermore, the rationale for using one reference level over another is unclear. Smith et al. (1986) claim that ERBE used a flux reference level of 30 km as a ''compromise'' between the level where the radiation comes from (relatively low altitudes) and the ''important'' amount of radiation from the upper levels of the atmosphere.

A reasonable question to ask, therefore, is whether there exists a flux reference level that is most appropriate for estimating the earth's radiation budget. Related to this is the question of what flux reference level to use when comparing satellite-derived TOA fluxes with plane-parallel climate model calculations [e.g., from a general circulation model (GCM)]. Since a plane-parallel climate model assumes the earth–atmosphere is horizontally infinite, the notion of a reference level is irrelevant in a plane-parallel world.

To address the first question, it is useful to consider the simplest form of the radiation budget of the earth:

$$\frac{S_o}{4}(1 - \alpha) = F^a, \tag{9}$$

where S_o is the solar constant ($=1365$ W m^{-2}), α is the planetary albedo, and F^a is the globally averaged absorbed SW flux. If the planet is in radiative balance, F^a is equal to the globally averaged outgoing LW flux. This simple view assumes the earth–atmosphere system intercepts solar radiation much like a ''billiard ball'' of some fixed diameter suspended in a vacuum. That is, all of the intercepted solar radiation below a reference level corresponding to the outer diameter of the billiard ball is either completely reflected or absorbed (Fig. 6a), and all of the solar radiation incident above the reference level is completely transmitted. If the reference level is moved to a height h above the surface, Eq. (9) is not applicable since it ignores the fraction of incident solar radiation below h that is transmitted (Fig. 6b). In that case, a more suitable form of the radiation budget equation is

$$\frac{S_o}{4}(1 - \alpha_h - t_h) = F_h^a, \tag{10}$$

where t_h represents the fraction of incident solar radiation that is transmitted below h. If h is defined at a reference level where all of the radiation escaping the planet is accounted for, the inverse-square law [Eq. (7)] can be used to provide an expression for the radiation budget at an arbitrary flux reference level x as follows:

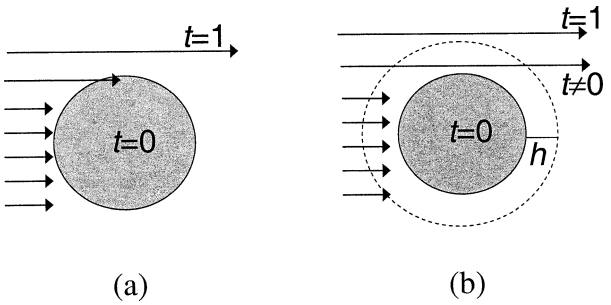

FIG. 6. Schematic of the earth–atmosphere system intercepting solar radiation as a billiard ball of some fixed diameter. (a) A surface reference level is assumed, so all of the intercepted solar radiation below that reference level is either completely reflected or absorbed. (b) The reference level is raised to a height h above the surface, so part of the incident solar radiation is transmitted horizontally through the planet.

$$\frac{S_o}{4} - \left(\frac{r_e + h}{r_e + x}\right)^2 (F_h^r + F_h^a) - t_h' \frac{S_o}{4} = 0, \tag{11}$$

where $F_h^r = (S_o/4)\alpha_h$ is the reflected flux. Using Eq. (10) to express F_h^a in terms of α_h and t_h, and substituting this into Eq. (11) yields an expression for t_h' in terms of t_h:

$$t_h' = 1 - \left(\frac{r_e + h}{r_e + x}\right)^2 (1 - t_h). \tag{12}$$

As the reference level x is decreased, the magnitude of the reflected and absorbed fluxes [second and third terms in Eq. (11)] increase, and the magnitude of the last term in Eq. (11) decreases. At some reference level $x = d$, the last term in Eq. (11) reaches zero, and Eq. (11) reduces to a form similar to Eq. (9). From Eq. (12), this occurs at

$$d = (r_e + h)\sqrt{1 - t_h} - r_e. \tag{13}$$

At the reference level d, there is no need to explicitly account for the transmission term in the radiation budget equation. At that reference level, the radiation budget of the earth is analogous to that for a hypothetical planet with an atmosphere of thickness d that reflects or absorbs all incident solar radiation below d, and transmits all incident solar radiation above d. In this context, therefore, d corresponds to the effective radiative ''top of the atmosphere'' for the planet.

When no atmosphere is present, $d = 0$ km, and $t_h' = t_x^{\text{no atm}}$, where $t_x^{\text{no atm}}$ is given by

$$t_h^{\text{no atm}} = \frac{\pi(r_e + h)^2 - \pi r_e^2}{\pi(r_e + h)^2} = 1 - \left(\frac{r_e}{r_e + h}\right)^2. \tag{14}$$

When the atmosphere is included, the effective ra-

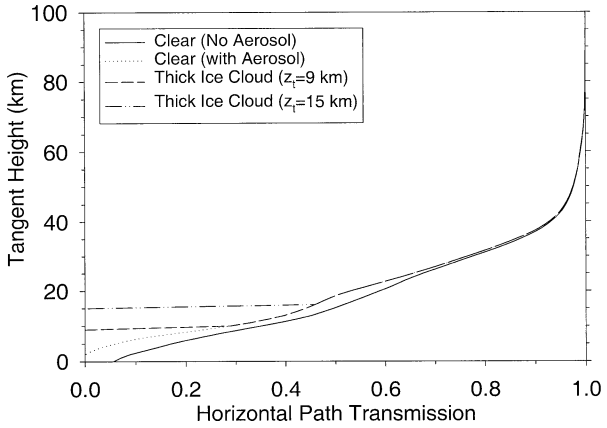

FIG. 7. MODTRAN calculations of spectrally integrated horizontal path transmission through the atmosphere at different tangent heights above the earth's surface.

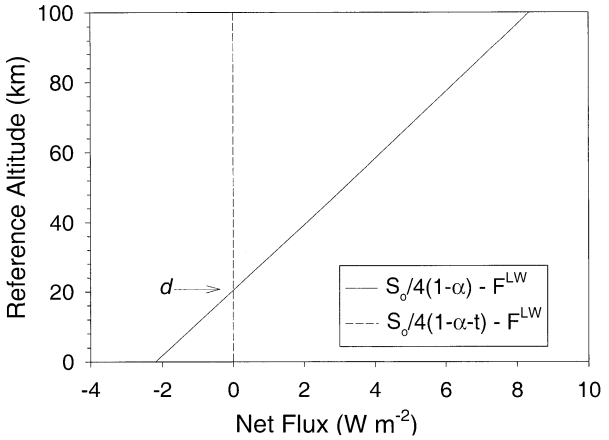

FIG. 8. Net flux at different reference levels evaluated by ignoring the transmitted flux at each reference level (solid line) and by explicitly accounting for the transmitted flux (dashed line).

diative TOA (d) lies above the surface since the atmosphere now attenuates part of the incoming solar radiation. In order to estimate t_h and d when an atmosphere is present, MODTRAN (Kniezys et al. 1996) calculations of spectrally integrated horizontal path transmission through the atmosphere at different tangent heights above the earth's surface are performed (Fig. 7). Table 1 summarizes the properties for the five cases considered. The first four use atmospheric profiles of temperature, pressure, and atmospheric gases based on the tropical model atmosphere of McClatchey et al. (1972), while the fifth case uses subarctic winter profiles. When included, aerosols are present throughout the atmosphere: marine aerosols are used in the boundary layer between 0 and 2 km, tropospheric aerosols lie between 2 and 10 km, background stratospheric aerosols lie between 10 and 30 km, and meteoric dust lies between 30 and 100 km. Assuming each of the cases in Table 1 covers the entire globe, an estimate of t_h for each case can be determined from the following:

$$t_h = \frac{\int_0^{r_e+h} 2\pi r t(r)\, dr}{\pi(r_e + h)^2}, \tag{15}$$

where $t(r)$ is the spectrally integrated horizontal path transmission (Fig. 7) determined from

$$t(r) = \frac{\int_0^{\infty} t_\lambda(r) S_\lambda\, d\lambda}{\int_0^{\infty} S_\lambda\, d\lambda}, \tag{16}$$

and S_λ is the spectral solar irradiance. For the five cases in Table 1, t_h ranges from 2.354×10^{-2} to 2.546×10^{-2}. This means that approximately 8 W m^{-2} [$=(S_o/4) \times t_h$] is transmitted through the first 100 km of the earth–atmosphere. The difference in transmitted energy between the extreme cases (cases 4 and 5) is approximately $341 \times (2.546 - 2.354) \times 10^{-2}$ or 0.66 W m^{-2}. By comparison, if there were no atmosphere, approximately 10.5 W m^{-2} would be transmitted below 100 km.

For the cases in Table 1, d ranges from 17.1 to 23.4 km. The subarctic winter atmosphere attenuates the least amount of solar radiation, and therefore d occurs at the lowest level. While it is possible to adjust d as a function of scene type when evaluating TOA fluxes from actual measurements, it is simpler to choose a fixed value of 20 km for all scenes. Based on the extreme cases considered in Table 1, the error in net radiation caused by neglecting the transmission term and using a global 20-km reference level remains <0.35 W m^{-2}.

Figure 8 shows an example of the ''net flux'' as a function of reference level for the spectrally integrated

TABLE 1. Description of properties for the cases used in MODTRAN simulations of horizontal path transmission through the atmosphere.

Case	Profiles	Aerosol	Cloud	t_h ($\times 10^{-2}$)	d (km)
1	Tropical	No	No	2.503	18.5
2	Tropical	Yes	No	2.446	20.5
3	Tropical	Yes	Thick ice Z_t = 9 km	2.423	21.1
4	Tropical	Yes	Thick ice Z_t = 15 km	2.354	23.4
5	Subarctic winter	No	No	2.546	17.1

horizontal path transmission in case 2 of Table 1, evaluated by ignoring the transmitted flux at all reference levels (solid line), and explicitly accounting for the transmitted flux at all levels (dashed line). These calculations assume a planet in radiative balance that absorbs 70% of the solar radiation and transmits 2.446% below 100 km. If a reference level of 100 km were assumed, ignoring the transmitted flux would lead to an apparent net flux of $\approx$8 W m^{-2}. In contrast, at a reference level near 20 km, where the condition in Eq. (13) is satisfied, the simple form of the radiation budget equation given by Eq. (9) provides the correct net flux of zero. In this example, therefore, it would be preferable to choose a reference level at 20 km rather than 100 km since there is no need to explicitly specify what the transmitted flux is for the 20-km reference level in order to correctly determine the net flux.

Since the plane-parallel climate model approximation assumes the earth–atmosphere system is horizontally infinite, the concept of flux reference level as defined in the present study is not relevant. Therefore, at what flux reference level should satellite-derived TOA fluxes be defined when comparing with plane-parallel climate model flux calculations? Since a plane-parallel model atmosphere is horizontally infinite, the horizontal transmission term in the radiation budget equation is zero. Given that a zero transmission term for a finite earth only occurs when the reference level is close to 20 km, it follows that the 20-km reference level is also the most appropriate reference level to define satellite-derived TOA fluxes when comparing with plane-parallel climate model calculations. At any other reference level, the model calculations would have to explicitly account for the extra term in the radiation budget equation [last term in Eq. (11)].

4. ERBE approach

The methodology used to construct ERBE ADMs is outlined in Suttles et al. (1988, 1989). The ERBE ADMs were constructed using *Nimbus-7* ERB scanner data with scene identification from the *Nimbus-7* Temperature–Humidity Infrared Radiometer (THIR) and the Total Ozone Mapping Spectrometer (TOMS; Taylor and Stowe 1984; Stowe et al. 1988). TOA fluxes for individual ADM scene types were determined using a surface FOV reference level. Consequently, radiance contributions by the earth's annulus were not accounted for in these models. The ADMs were applied to ERBE radiance measurements on *NOAA-9, -10,* and *ERBS* using scene identification based on the maximum likelihood technique (MLE; Wielicki and Green 1989). When the ADMs were applied, viewing geometry and footprint geolocation were defined at a 30-km FOV reference level instead of the surface FOV reference level.

Using a viewing geometry defined at the 30-km FOV reference level to apply ADMs defined at the surface FOV reference level introduces a slight bias in the estimated TOA fluxes since it means that the ADM value used to estimate flux is evaluated at a viewing zenith angle that is too small compared to what it would be at the surface FOV reference level. To estimate the uncertainty, Fig. 9 shows the approximate error in daily averaged LW and SW fluxes as a function of 30-km viewing zenith angle. The errors were determined using tropical average all-sky LW and SW ADMs constructed from 9 months of CERES/TRMM data. Assuming the models are representative of average conditions, the LW flux determined using viewing geometry at a 30-km reference level is underestimated by $\approx$0.2 W m^{-2}, on average, but can reach 0.9 W m^{-2} at $\theta = 70°$. In the SW, the flux is overestimated by $\approx$0.4 W m^{-2}, on average, but reaches 1.4 W m^{-2} at $\theta = 70°$. The sign of the flux bias is opposite for SW and LW because, on average, LW ADM anisotropic factors decrease with viewing zenith angle (limb darkening), while SW ADM anisotropic factors increase with viewing zenith angle (limb brightening). Systematically underestimating the viewing zenith angle thus leads to an overestimation (underestimation) of the anisotropic factor (flux) in the LW, while the opposite occurs in the SW. Since the SW and LW flux errors are of opposite sign and have approximately the same magnitude, the effect of these errors on net radiation is negligible.

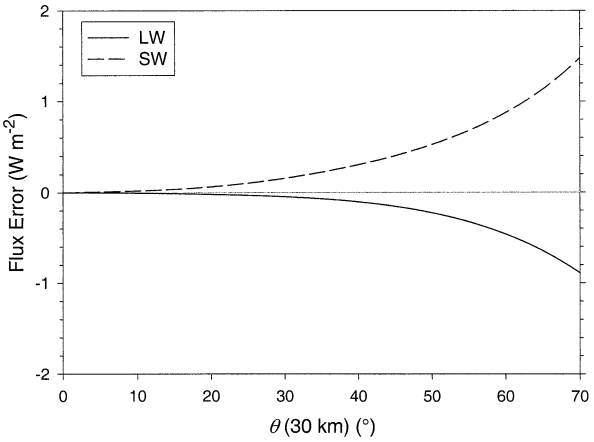

FIG. 9. Estimated bias in ERBE TOA flux due to the use of a 30-km FOV reference level to apply ADMs defined using a surface FOV reference level.

The use of a 30-km reference level for defining the latitude–longitude position of ERBE FOVs (or footprint geolocation) also has an important effect on the interpretation of the measurements. When a cloud or surface feature is observed from an oblique viewing zenith angle, the reported FOV latitude–longitude position on the ERBE or CERES ERBE-like product will be displaced relative to the actual latitude–longitude position of the cloud or surface feature. To illustrate, Fig. 10 shows a schematic of a cloud at a height h (at point B) observed at viewing zenith angle θ_{30} relative to the 30-km reference level (point C). Here, the reported FOV position

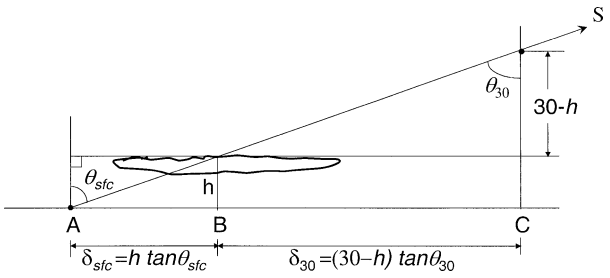

FIG. 10. Schematic illustrating geolocation error for a cloud located at B caused by using 30-km (C) and surface (A) reference levels to define the location of a measurement.

is displaced from the true position of the cloud by a distance of approximately $(30 - h)\tan\theta_{30}$. For a viewing zenith angle of 70°, a cloud near the surface would be displaced by as much as 82 km from the FOV position.

5. CERES approach

Instantaneous TOA fluxes from CERES instruments aboard the *TRMM*, *Terra*, and *Aqua* spacecraft appear on two data products: the ''ERBE-like'' product, and the Single Scanner Footprint (SSF) product. As its name implies, the CERES ERBE-like product consists of CERES measurements processed using algorithms developed during the ERBE experiment (Wielicki et al. 1996). The CERES SSF product combines CERES and imager measurements to provide coincident and collocated cloud and radiation parameters for every CERES footprint within the imager swath. To take advantage of the improved scene identification provided by the higher-resolution imager measurements, a new set of CERES SW and LW ADMs are being developed for the CERES instruments on each of the three spacecraft. The new ADMs are stratified into several scene types according to imager-based parameters that have a strong influence on the anisotropy of scenes (e.g., cloud fraction, cloud optical depth, phase, etc.). For now, we defer a comprehensive description of the new CERES ADM scene types to a future paper.

To construct the new CERES ADMs, an approach very similar to that outlined in section 2 is used. Radiances for a given imager-based scene type are collected from several months of data, sorted into angular bins, and averaged. The radiances are then integrated directly over the upward hemisphere to determine the ADM flux using a 100-km FOV reference level to account for the contribution of radiances above the earth's tangent point. Radiance contributions above the earth's tangent point are inferred from MODTRAN calculations for a molecular atmosphere. Since the viewing geometry and the latitude–longitude of CERES footprints and imager pixels on the CERES SSF are defined at the surface reference level, for consistency, the CERES ADMs are also defined at the surface reference level by setting $h = 0$ in Eq. (8). However, instantaneous TOA fluxes estimated from the CERES radiances are adjusted to the 20-km flux reference level in order to correspond with the effective ''radiative'' TOA.

By defining the latitude–longitude position of CERES FOVs at the surface, footprint geolocation errors on the CERES SSF are dramatically reduced compared to ERBE. A cloud at a height h (point B in Fig. 10) observed at viewing zenith angle θ_{sfc} relative to the surface (point A in Fig. 10) is displaced by a distance $h\tan\theta_{sfc}$ from the reported FOV position. While the position of objects located at the surface are consistent with the FOV position, a cloud at 10 km will be displaced by 28 km relative to the FOV position. By comparison, a cloud at 10 km would be displaced by 55 km from the reported FOV position in the ERBE or CERES ERBE-like product.

6. Summary and conclusions

To estimate the earth radiation budget from satellite radiances, the radiances must first be converted to TOA fluxes. ERBE and CERES use empirical angular distribution models for scene types having distinct anisotropic characteristics. To construct an ADM, radiances for predefined scene types are collected from several months of data, sorted into angular bins, and averaged. The mean radiances are then integrated over the upward hemisphere to provide the TOA flux for each ADM class. ADM anisotropic factors are determined from the ratio of the isotropic flux in each angular bin (based on the bin's mean radiance) to the TOA flux for the appropriate ADM class. To determine the TOA flux for an ADM class by direct integration of the mean radiances, the FOV reference level—which defines the level where a measurement's sun–earth–observer viewing geometry is located—must lie well above the earth's surface (e.g., 100 km). This ensures that all radiation contributions (including the radiation escaping the planet along slant paths above the earth's tangent point) are accounted for. If the FOV reference level is defined at an altitude that is too low (such as the surface reference level), TOA fluxes for most scene types will be systematically underestimated by 1–2 W m^{-2}.

Since TOA flux varies with distance from the center of the earth according to the inverse-square law, a reference level is also needed to define TOA flux. In order to determine the most appropriate flux reference level for estimating the earth's radiation budget, the radiation budget equation is expressed as a function of reference level, accounting for the fraction of incident solar radiation that is transmitted horizontally through the atmosphere. As the reference level is decreased, the reflected and absorbed solar fluxes increase according to the inverse-square law, whereas the transmitted flux decreases in order to maintain a balance between the incoming solar radiation and the sum of the reflected, absorbed, and transmitted fluxes. At some reference lev-

el *d*, the transmission term vanishes, and the radiation budget reduces to a balance between incoming solar radiation and the reflected and absorbed solar fluxes. At that reference level, the radiation budget of the earth is analogous to that for a hypothetical planet with an atmosphere of thickness *d* that reflects or absorbs all incident solar radiation below *d*, and transmits all incident solar radiation above *d*. In this context, therefore, *d* corresponds to the effective radiative ''top of the atmosphere'' for the planet. Of course, if there were no atmosphere, the effective radiative top of the atmosphere would correspond to the earth's surface. Adding an atmosphere that attenuates solar radiation raises the effective radiative top of the atmosphere to approximately 20 km above the surface, based on MODTRAN simulations for several different atmospheric scenarios. Therefore, from these results, the 20-km reference level appears to be the most appropriate flux reference level for defining satellite-based TOA fluxes for earth radiation budget studies.

Since climate models generally use a plane-parallel approximation to estimate TOA fluxes and the earth radiation budget, there is no need to specify a reference level, and horizontal transmission of solar radiation is assumed to be zero in the radiation budget equation. When the planet's finite geometry is taken into consideration, the transmission contribution drops out of the radiation budget equation only when fluxes are defined at the 20-km flux reference level. Consequently, to compare model results with observations, fluxes inferred from the observations should also be defined at the 20-km reference level.

Acknowledgments. The authors would like to thank Dr. Thomas P. Charlock and Mr. Fred G. Rose for their many helpful comments. This research was funded by the Clouds and the Earth's Radiant Energy System (CERES) project under NASA Grant NAG-1-2318. Partial support was also provided under NASA Grant NAG-1-1096.

REFERENCES

Barkstrom, B. R., 1984: The Earth Radiation Budget Experiment (ERBE). *Bull. Amer. Meteor. Soc.,* **65,** 1170–1186.

Diner, D. J., and Coauthors, 1999: New directions in earth observing: Scientific applications of multiangle remote sensing. *Bull. Amer. Meteor. Soc.,* **80,** 2209–2228.

House, F. B., A. Gruber, G. E. Hunt, and A. T. Mecherikunnel, 1986: History of satellite missions and measurements of the Earth radiation budget (1957–84). *Rev. Geophys. Res.,* **24,** 357–377.

Jacobowitz, H., R. J. Tighe, and the NIMBUS 7 ERB Experiment Team, 1984: The earth radiation budget derived from the *NIMBUS 7* ERB Experiment. *J. Geophys. Res.,* **89,** 4997–5010.

Kneizys, F. X., and Coauthors, 1996: The MODTRAN 2/3 Report and LOWTRAN 7 Model. Phillips Laboratory, Geophysics Directorate, Hanscombe AFB, 261 pp.

Loeb, N. G., K. J. Priestley, D. P. Kratz, E. B. Geier, R. N. Green, B. A. Wielicki, P. O'R. Hinton, and S. K. Nolan, 2001: Determination of unfiltered radiances from the Clouds and the Earth's Radiant Energy System (CERES) instrument. *J. Appl. Meteor.,* **40,** 822–835.

McClatchey, R. A., R. W. Fenn, J. E. A. Selby, P. E. Volz, and J. S. Garing, 1972: Optical properties of the atmosphere. 3d ed. Air Force Cambridge Research Laboratory Paper AFCRL-72-0497, Environmental Research Paper 411, Air Force Cambridge Research Laboratory, Bedford, MA, 103 pp.

Smith, G. L., 1994: Effects of time response on the point spread function of a scanning radiometer. *Appl. Opt.,* **33,** 7031–7037.

——, R. N. Green, E. Raschke, L. M. Avis, J. T. Suttles, B. A. Wielicki, and R. Davies, 1986: Inversion methods for satellite studies of the earth radiation budget: Development of algorithms for the ERBE mission. *Rev. Geophys.,* **24,** 407–421.

Stowe, L. L., C. G. Wellemeyer, T. F. Eck, H. Y. M. Yeh, and the Nimbus-7 Cloud Data Processing Team, 1988: *Nimbus-7* global cloud climatology. Part I: Algorithms and validation. *J. Climate,* **1,** 445–470.

Suttles, J. T., and Coauthors, 1988: Angular radiation models for earth–atmosphere systems. Vol. I. Shortwave radiation. NASA Rep. RP-1184, NASA, Washington, DC, 147 pp.

——, R. N. Green, G. L. Smith, B. A. Wielicki, I. J. Walker, V. R. Taylor, and L. L. Stowe, 1989: Angular radiation models for earth–atmosphere systems. Vol. II. Longwave radiation. NASA Rep. RP-1184, NASA, Washington, DC, 87 pp.

Taylor, V. R., and L. L. Stowe, 1984: Reflectance characteristics of uniform Earth and cloud surfaced derived from *Nimbus 7* ERB. *J. Geophys. Res.,* **89,** 4987–4996.

Thomas, G. E., and K. Stamnes, 1999: *Radiative Transfer in the Atmosphere and Ocean.* Cambridge University Press, 527 pp.

Wielicki, B. A., and R. N. Green, 1989: Cloud identification for ERBE radiation flux retrieval. *J. Appl. Meteor.,* **28,** 1133–1146.

——, B. R. Barkstrom, E. F. Harrison, R. B. Lee III, G. L. Smith, and J. E. Cooper, 1996: Clouds and the Earth's Radiant Energy System (CERES): An earth observing system experiment. *Bull. Amer. Meteor. Soc.,* **77,** 853–868.